

---

# FILAMENTARY AND PLANAR STRUCTURES IN GRAVITATION AND OBSERVABLE EFFECTS

G. IOVANE, E. LASERRA<sup>1</sup>

UDC 539

© 2004

Dipartimento di Ingegneria dell'Informazione e Matematica Applicata,  
Università di Salerno

(Italy; e-mail: geriov@sa.infn.it),

<sup>1</sup>Dipartimento di Matematica e Informatica, Università di Salerno

(Italy; e-mail: laserra@unisa.it)

---

A waveguiding effect is considered in respect to the large-scale structure of the Universe. In particular, we consider filamentary and planar large-scale structures as possible refraction channels for electromagnetic radiation coming from cosmological structures. Thanks to a numerical simulation by this hypothesis and the analytical model, it is possible to explain the quasar luminosity distribution and, in particular, the presence of "twin" or "brother" objects. The method and details of the simulation are given.

---

## 1. Introduction

The gravitational lensing effects can be explained by considering the action of a weak gravitational field deflecting the light rays which come from a fixed source [1, 2]. In other words, it is possible to define a refraction index connected to the Newtonian gravitational field. There are other mechanisms, like as waveguiding, which are described by analogous equations. Then we show how the analogy with the gravitational field can be extended also to these processes taking into account a sort of "nonlinearity" in gravitational lensing.

Let us suppose that the matter distributions in the Universe may produce a gravitational potential inducing the channeling effect. As we will show, such an effect could explain several anomalies which are hard to connect to standard gravitational lensing models, like, e.g. the existence of objects with the same spectrum and redshift, but placed in the sky at large angular distances (e.g. twins). The huge luminosity of quasars could be explained by using cosmological structures as well [3, 4]. In principle, all primordial topological defects as cosmic strings, textures, and domain walls could be evolved so that today they can trap electromagnetic or gravitational radiation [5–7].

This gravitational waveguiding effect has the same physical reason of the gravitational lensing effect, which account for the light deflection given by a gravitational

field acting like a refraction medium [8]. However, there are some substantial differences: the gravitational lenses are usually compact objects. On the contrary, the density can be low in these gravitational channels; moreover, the radiation is deflected by a lens, but it does not pass through the object, while the light have to travel "inside" the matter distribution in the case of gravitational channels.

The existence of the waveguiding effect could explain the huge luminosity of very far objects like quasars. Another effect could be the generation of twins and brothers. In other words, an observer could detect two images of the same object: the real image and the one caught by the gravitational channel.

From a theoretical point of view, the matter distribution should locally produce an effective gravitational potential of the form  $\Phi(r^2) \sim r^2$ .

It is worth to note that the specific form of  $r$  (and then of the effective gravitational potential) depends on a particular symmetry of the system. We assume an almost constant density  $\rho$  which is substantially different with respect to the background.

The planar or filamentary distributions, essentially connected to a gradient of matter density, could be generated at the contact surfaces among several expanding bubbles. This point of view has a relevant connection with the geometry of the Universe and the noncommutative geometry [9], with Cantorian geometry [10], and with the Penrose–Mackay tiling [11].

The paper is organized as follows. In Sec.2, a theoretical model for gravitational waveguides is developed. Sec.3 is devoted to the discussion of the early cosmological phase transition, topological defects, and possible connections to the today observed large-scale structures. In Sec. 4, we present a simulation by which we try to explain the luminosity distribution of quasars assuming that a part of them has been "twinned" because the radiation emitted from them has undergone a channelling process by intervening filamentary or

planar large-scale structures. The results and conclusions are drawn in Sec.5.

## 2. The Gravitational Waveguide Model

Let us consider the Maxwell equations to describe the behaviour of an electromagnetic field, without sources and in the presence of a gravitational field [1],

$$\begin{aligned} \frac{\partial F_{\alpha\beta}}{\partial x^\gamma} + \frac{\partial F_{\beta\gamma}}{\partial x^\alpha} + \frac{\partial F_{\gamma\alpha}}{\partial x^\beta} &= 0; \\ \frac{1}{\sqrt{-g}} \frac{\partial}{\partial x^\beta} (\sqrt{-g} F^{\alpha\beta}) &= 0, \end{aligned} \quad (1)$$

where  $F^{\alpha\beta}$  is the electromagnetic field tensor and  $\sqrt{-g}$  is the determinant of the four-dimensional metric tensor. Channeling solutions can be obtained by reducing the Maxwell equations in a medium to the scalar Helmholtz equation for the fields  $\mathbf{E}$  and  $\mathbf{H}$ . For the electrical field, after the Fourier transformation, we can write

$$\Delta \mathbf{E}_\omega(\mathbf{r}) + \frac{\omega^2}{c^2} n^2(\omega, \mathbf{r}) \mathbf{E}_\omega(\mathbf{r}) = 0 \quad (2)$$

where  $\omega$  is the frequency of the given Fourier component<sup>1</sup>. A general solution has the form

$$\begin{aligned} \mathbf{E}_\omega(\mathbf{r}) &= \mathbf{E}_\omega^{(0)}(\mathbf{r}) + \int \mathcal{G}(\mathbf{r}, \mathbf{r}', \omega) \times \\ &\times \nabla \left[ \frac{\mathbf{E}_\omega^{(0)}(\mathbf{r}) \nabla \varepsilon(\omega, \mathbf{r})}{\varepsilon(\omega, \mathbf{r})} \right] d\mathbf{r}, \end{aligned} \quad (3)$$

where  $\mathcal{G}$  is the Green function for the equation

$$\left[ \Delta + \frac{\omega^2}{c^2} n^2(\omega, \mathbf{r}) \right] G(\mathbf{r}, \mathbf{r}', \omega) = \delta(\mathbf{r} - \mathbf{r}'). \quad (4)$$

This is a Schrödinger-like equation for the energy constant  $E = 0$ . In fact, if we write down the Hamiltonian operator  $\hat{\mathcal{H}} = -\frac{1}{2}\Delta + U(\mathbf{r})$ , with  $\hbar = m = 1$  and  $U(\mathbf{r}) = -2\frac{\omega^2}{c^2} n^2(\omega, \mathbf{r})$ , a fully analogy between the two problems is obtained.  $U(\mathbf{r})$  assumes the role of the Newtonian potential  $\Phi(\mathbf{r})$ .

Let us consider the scalar Helmholtz equation for an arbitrary monochromatic component of the electric field,

$$\frac{\partial^2 E}{\partial z^2} + \frac{\partial^2 E}{\partial x^2} + \frac{\partial^2 E}{\partial y^2} + k^2 n^2(\mathbf{r}) E = 0, \quad (5)$$

where  $k$  is the wavenumber. The  $z$  coordinate can be considered as the longitudinal one and it can measure

the space distance along the structure produced by a mass distribution with an optical axis.

Let us consider now a solution of the form

$$\begin{aligned} E &= n_0^{-1/2} \Psi \exp \left( ik \int^z n_0(z') dz' \right); \\ n_0 &\equiv n(0, 0, z), \end{aligned} \quad (6)$$

where  $\Psi(x, y, z)$  is a slowly varying spatial amplitude along the  $z$  axis, and  $\exp(iknz)$  is a rapidly oscillating phase factor. It is clear that the beam propagates along the  $z$  axis. We rewrite the Helmholtz equation neglecting the second-order derivative with respect to the longitudinal  $z$  coordinate and obtain a Schrödinger-like equation for  $\Psi$ :

$$\begin{aligned} i\lambda \frac{\partial \Psi}{\partial \xi} &= -\frac{\lambda^2}{2} \left( \frac{\partial^2 \Psi}{\partial x^2} + \frac{\partial^2 \Psi}{\partial y^2} \right) + \\ &+ \frac{1}{2} [n_0^2(z) - n^2(x, y, z)] \Psi, \end{aligned} \quad (7)$$

where  $\lambda$  is the electromagnetic radiation wavelength and  $\xi = \int^z \frac{dz'}{n_0(z')}$  is a new normalized variable with respect to the refraction index. It is interesting to stress that the role of Planck constant is assumed by  $\lambda$ .

At this point, it is worth to note that if one has a distribution of matter in the form of a cylinder or a sphere with a constant (dust) density, the gravitational potential inside has a parabolic profile providing channeling effects for electromagnetic radiation analogous to the self-foc optical waveguides realized in optical fibers. In this case, the Schrödinger-like equation describes a two-dimensional quantum harmonic oscillator, for which solutions exist in the form of Gauss-Hermite polynomials (see, e.g., [12]).

The channeling effect depends explicitly on the potential shape: The radiation from a remote source is not attenuated if  $U \sim r^2$ ; this situation is realized supposing a "planar" mass distribution ( $r = x$ ) or a filamentary distribution ( $r = \sqrt{x^2 + y^2}$ ) with constant density. In other words, if the radiation, travelling from some source, undergoes the channelling effect, it is not attenuated like  $1/R^2$  as usual, but it is conserved, in some sense; this fact means that the source brightness will turn out to be much stronger than the brightness of analogous objects located at the same distance.

<sup>1</sup>A similar equation holds for the magnetic field.

### 3. Candidates for Cosmological Refraction Channels

Early structures, resulting from inflationary phase transitions, could be good candidates to implement the above filamentary or planar structures acting as cosmological refraction channels. Essentially, if the primordial universe undergoes a first- or second-order phase transition, such a transition takes place on a short-time scale ( $\tau < H^{-1}$ ), and it will lead to correlation regions, inside of which the value of a certain scalar field  $\varphi$  (the inflaton which leads the dynamics) is approximately constant, but outside  $\varphi$  ranges randomly over the vacuum manifold. In the simplest case, for a Ginzburg–Landau-like potential of the form

$$V(\varphi) = \frac{\lambda}{4} (\varphi^2 - \varphi_0^2)^2, \quad (8)$$

the correlation regions are separated by domain walls, regions in space where  $\varphi$  leaves the vacuum manifold  $\mathcal{M}$  and where, therefore, the potential energy is localized. This energy density can act as a seed for structure.

There are various types of local and global topological defects [13] (regions of trapped energy density) depending on the number of real components of  $\varphi$  (being, in general,  $\varphi^2 = \sum_{i=1}^n \varphi_i^2$ ). In the case of domain walls,  $n = 1$ .

The more rigorous mathematical definition refers to the homotopy of  $\mathcal{M}$ . The words “local” and “global” refer to whether the symmetry, which is broken, is a gauge or global symmetry. In the case of local symmetries, the topological defects have a well-defined core, outside of which  $\varphi$  contains no energy density in spite of nonvanishing gradients  $\nabla\varphi$ ; the gauge field can absorb the gradient, i.e.  $D_\mu\varphi = 0$  when  $\partial_\mu\varphi \neq 0$ . Global topological defects, however, have long-range density fields and forces.

Practically, topological defects can be classified by their topological characteristic which, in terms of the scalar field  $\varphi$ , depends on the number of real components.

Point-like defects give monopoles, linear defects give cosmic strings, surface-like defects are domain walls, hypersurface-like defects, but not properly topological defects are textures.

In principle, all these structures can be seeds for large-scale structures depending on the cosmological model we adopt. Taking into account realistic scenarios, the best candidates seem to be cosmic strings.

Furthermore, any first-order phase transition proceeds via bubble nucleation so that invoking the

filamentary and planar structures for channeling effects is reasonable (local surface portions of large bubbles can be approximated to planar structures).

For example, cosmic strings easily realize the condition to obtain a Newtonian potential useful, as discussed above, to produce a gravitational refraction channel. In fact, in the weak energy limit approximation, these topological defects are described internally by the Poisson equation  $\nabla^2\Phi = \rho_0$  and externally by  $\nabla^2\Phi = 0$ , where  $\rho_0$  is a constant. The condition on the density gradient is naturally recovered. Another useful feature is that they act as gravitational lenses after the quasar formation [6, 14]. Immediately we get, internally,  $\Phi \sim r^2$  and, by the dynamical evolution of the Universe, strings can evolve into structures with lengths of the order  $\sim 100$  Mpc. However, also after evolution, strings remain “wires” and then, in order to get the cylindrical structures which we need for gravitational channels (e.g. a filament of galaxies), we have to invoke further processes where strings are seeds to cluster matter at large scales.

Furthermore, the motion of cosmic strings with respect to the background produces wakes and filaments which are able to evolve into large-scale structures like clusters or filaments of galaxies [15].

All these arguments, as is well known, are hypotheses for the large-scale structure formation.

Our issue is now to construct a reasonable model which, by channeling effects, could explain, in a simple way, the huge luminosity of quasars and twin effects in gravitational lensing.

### 4. The Model and Simulation

To fix the ideas, let us estimate how the electric field propagates into an ideal filament whose internal potential is

$$U(r) = \frac{1}{2}\omega^2 r^2, \quad \omega^2 = \frac{4\pi G\rho}{c^2}. \quad (9)$$

A spherical wave from a source has the form

$$E = (1/R)\exp(ikR). \quad (10)$$

In the paraxial approximation, Eq. (11) becomes

$$E(z, r) = \frac{1}{z} \exp\left(ikz + \frac{ikr^2}{2z} - \frac{r^2}{2z^2}\right), \quad (11)$$

where we used the expansion

$$R = (z^2 + r^2)^{1/2} \approx z \left(1 + \frac{r^2}{2z^2}\right), \quad r \ll z. \quad (12)$$

It is realistic to assume  $n_0 \simeq 1$ , so that  $\xi = z$ .

Let us consider now that the starting point of the gravitational channel of length  $L$  is at a distance  $l$  from a source shifted by a distance  $a$  from the structure longitudinal axis in the  $x$  direction. The amplitude of the field  $E$  entering the channel is

$$\Psi_{\text{in}} = \frac{1}{l} \exp \left[ \frac{ikl - 1}{2l^2} ((x - a)^2 + y^2) \right], \quad (13)$$

so that we have  $R = (l^2 + y^2 + (x - a)^2)^{1/2}$ . We can calculate the amplitude of the field at the exit of a filament by the equation

$$\begin{aligned} \Psi_{\text{out}}(x, y, l + L) &= \\ &= \int dx_1 dy_1 \mathcal{G}(x, y, l + L, x_1, y_1, l) \Psi_{\text{in}}(x_1, y_1, l), \end{aligned} \quad (14)$$

where  $\mathcal{G}$  is again the Green function for  $\Psi$ . In particular, taking into account the potential (9),  $\mathcal{G}$  is the propagator of the harmonic oscillator; then  $\Psi_{\text{out}}$  is a Gaussian integral that can be exactly evaluated. There are two interesting limits for  $\Psi_{\text{out}}$ .

If  $\omega l \ll 1$ , we have

$$\Psi_{\text{out}} = \frac{1}{i\lambda} \exp \left\{ -\frac{l + i\lambda}{2\lambda^2 l} [(x + a)^2 + y^2] \right\}, \quad (15)$$

which means that the radiation emerging from a point with coordinate  $(a, 0, 0)$  is focused near a point with coordinates  $(-a, 0, l + L)$  (that is, the radius has to be of the order of the wavelength). This means that, when the beam from an extended source is focused inside a gravitational channel at a distance  $L$ , an inverted image of the source is formed, having the very same geometric dimensions of the source. The channel “draws” the source closer to the observer since, if the true distance of the observer from the source is  $R$ , its image brightness will correspond to that of a similar source at the closer distance

$$R_{\text{eff}} = R - l - L. \quad (16)$$

In the opposite limit  $\omega l \gg 1$ , we have  $\text{tg}\omega L \rightarrow \infty$ , so that  $L \simeq \pi/\omega$ , that is, the shortest focal length of the gravitational channel is

$$L_{\text{foc}} = \sqrt{\frac{\pi c^2}{4G\rho}}. \quad (17)$$

It is relevant to note that the expression  $L_{\text{foc}}$  leads to a value of about 100 Mpc for a typical galactic density  $\rho_0 \sim 10^{-24} \text{ g/cm}^3$ . In other words, this can be assumed as a typical length for large-scale structures.

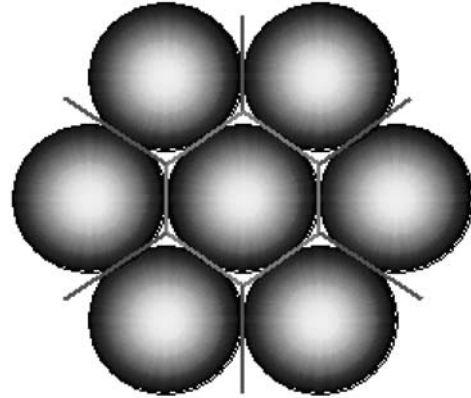


Fig. 1. Formation model of contacting planar structures

The major aim of our simulation is to perform a test about the possibility that twin or brother quasars could be explained by trapped and guided light, which was emitted by quasar sources and guided thanks to structures acting like channels. Moreover, the single quasar itself could be a typical object (a bulge of a standard galaxy) which appears so magnified thanks to the presence of channelling effects.

In our simulation, as discussed above, we can take into account a gravitational first-order phase transition, from which false vacuum bubbles nucleate inside a true vacuum cosmological background. Our fundamental assumption is that they cosmologically evolve giving rise to a cellular structure capable of yielding the observed large-scale structures [16]. After, we take into account also filamentary large-scale structures.

It is also important to note that, due to the cosmological expansion, the bubbles continue to grow even after they collide; this is the difference with models used in crystal growth such as the Voronoi model and the Johnson—Mehl ones, where crystals stop to grow in the direction of the neighbour one.

By simple geometric arguments, we can put, around a circle, other six circles with the same radius in a given area. If these circles are expanding, to minimize the space among them, they degenerate into hexagons. Fig. 1 shows the situation.

In other words, the density gradients of matter will be generated among the hexagons in the boundary regions. In the three-dimensional case, spheres will degenerate into dodecahedrons by forming a typical honeycomb structure with two-dimensional elementary pentagonal cells, whose surfaces will give rise to planar structures with matter density different from zero.

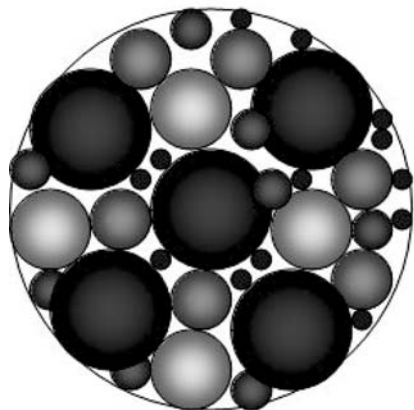


Fig. 2. A more realistic formation model of contacting planar structures

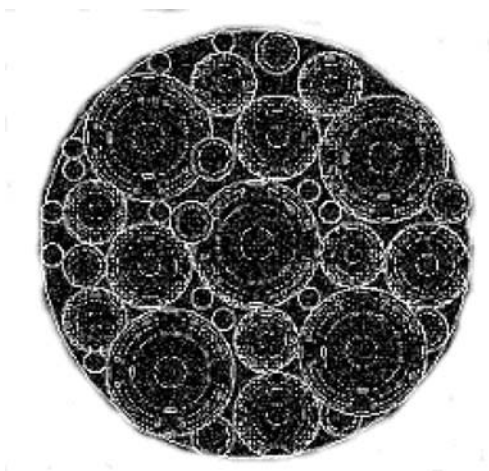


Fig. 3. A self-similar model for the formation of contacting planar structures

Finally, given an expanding universe, several dodecahedrons, remnants of a primordial gravitational phase transition, could yield a sort of honeycomb structure. The isotropy and homogeneity would be preserved at larger scales (size  $\sim 1000$  Mpc).

In this case, the formation of clustered galactic structures will be naturally due to the contact among several spheres, which would give rise to density gradients.

Such planar structures on contact surfaces could act as refraction channels, e.g. they could trap and guide the light due to the quasi-constant surface density; in this way, we should see an universe like that observed. To

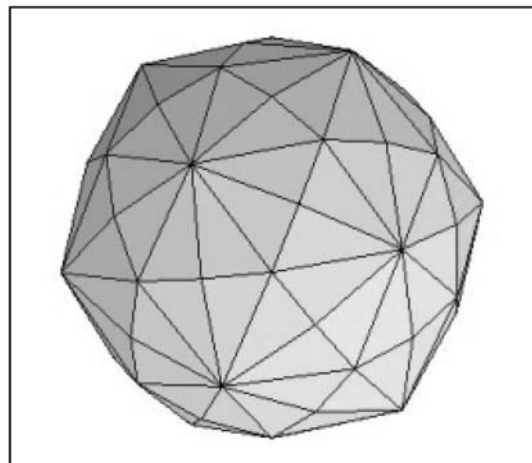


Fig. 4. Elementary cell like trapezoidal icositetrahedron

be more precise, we do not see an exact honeycomb, but a self-similar structure [9 – 11, 17] like those described in fractal models: in a more realistic model, we have to consider several spheres with different radii  $R_i$ . Then the generation model is like as in Fig. 2 and the self-similarity realizes a pattern like as in Fig. 3.

Then, we have not a perfect dodecahedron, but a more complicate polyhedron as, e.g., in Fig. 4. The dynamics will be governed by a symmetry breaking during the phase transition: the vacuum density could be different in different bubbles. Similar considerations can be done also for filamentary structures which act as refraction channels.

#### 4.1. Hypotheses and Previsions of the Simulation

Let us consider a universe model with an observed radius  $R_0 = 3000$  Mpc. Furthermore, let us assume 10000 quasars uniformly and isotropically distributed in this spherical space. The positions of the objects are fixed in a random way by using a random number generator. Moreover, the quasars are point-like objects. Furthermore, it is supposed that every single quasar can emit light in an isotropic way.

Between the refraction channels, we have to distinguish filamentary structures and planar structures.

We produce randomly distributed filamentary structures with a dimension of about 100 Mpc along the major axis and a shape like as a pseudo-cylinder. A typical simulated channel is shown in Fig. 5.

In particular, the channels of the model are built by five cylinders with a length in the range (1–20) Mpc and radius  $r$  in the range (1–100) Kpc. The positions of the channel starting points, that is, the centers of the first base circle in the first cylinder and the longitudinal axis of the cylinder are randomly generated.

There is a constraint on this generation, that is, the cylinders cannot collapse in a compact object.

Alternatively, we can have casually distributed planar structures acting like refraction channels, with linear dimensions of about 100 Mpc, on pentagonal surfaces.

In particular, in a universe with a radius  $R_0 = 3000$  Mpc, we can inscribe several pseudo-balls with a radius  $R_i$  such that the linear dimensions have an extension of about  $l_i = 100$  Mpc. This can be made in different ways:

1) Let us consider a circular sector with an angular spread of  $\pi/24 = 7.5^\circ$ ; by assuming that the linear extension of the structure has to be of 100 Mpc, we obtain:

$$100 \text{ Mpc} = l_i = \frac{\pi}{24} R_i \quad \rightarrow \quad R_i = 764 \text{ Mpc}. \quad (18)$$

In this case, we can inscribe  $n_{\text{balls}} = 60$  balls with radius  $R_i$  in the universe with radius  $R_0$ . Moreover, we have to calculate the error by assuming

$$2\pi R_i = 4800 \text{ Mpc}, \quad l = 100 \text{ Mpc} \quad \rightarrow$$

$$\rightarrow \quad \epsilon = \frac{l}{2\pi R_i} = 0.02 = 2\%.$$

2) By assuming a circular sector with an angular spread of  $\pi/18 = 10^\circ$ , we obtain

$$R_i = 573 \text{ Mpc}, \quad n_{\text{balls}} = 143, \quad \epsilon = 3\%.$$

3) By assuming a circular sector with an angular spread of  $\pi/12 = 15^\circ$ , we obtain

$$R_i = 382 \text{ Mpc}, \quad n_{\text{balls}} = 484, \quad \epsilon = 4\%.$$

4) By assuming a circular sector with an angular spread of  $\pi/10 = 18^\circ$ , we obtain

$$R_i = 318 \text{ Mpc}, \quad n_{\text{balls}} = 840, \quad \epsilon = 5\%.$$

5) By assuming a circular sector with an angular spread of  $\pi/9 = 20^\circ$ , we obtain

$$R_i = 286 \text{ Mpc}, \quad n_{\text{balls}} = 1154, \quad \epsilon = 6\%.$$

In the simulation, it is useful to implement an attenuation mechanism to make the model more

<sup>2</sup>in this step, the arrival points of coming out photons are evaluated

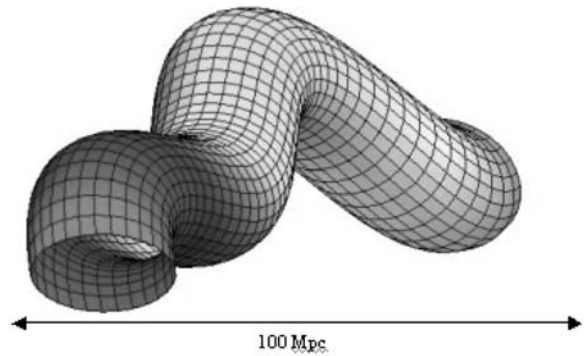


Fig. 5. A typical simulated channel

realistic. If the sources are at distances of the order of 1000 Mpc, since the luminosity decreases as  $R^{-2}$ , we assume that only fluxes large enough to survive to this physical cut can be detected as the channelling effects intervene. Otherwise they are completely absorbed by intergalactic media.

The next step is to verify how much light is trapped by the intervening channels and how many sources are lensed and then appear as twin images to the observer.

#### 4.2. Implementation and Results

The simulation was made by using the *New Object Visual Programming Technique* [18].

The simulation is built up by a main program which calls and manages a collection of subprocesses described as follows.

1) The first process is built up by 4 secondary sequences: i) the first one gives the quasar coordinates which are randomly generated; ii) the second one gives the photons coming out from quasars<sup>2</sup>; iii) the third one generates light rays at each quasar position; iv) the fourth one rejects all photons out of  $2R_0 = 6000$  Mpc (the boundary of our toy universe).

2) The second process regards the objects, whose light is picked up, trapped, and guided by the structures (it gives twinned quasars).

3) The third process has two sequences: i) the first one generates the refraction channel in random positions into the spherical volume representing the universe, while the second one evaluates the parameters to intersect the rays from quasars (this subprocess is completely equivalent to 1.5).

4) The fourth process evaluates the attenuation function for the light coming from quasars.

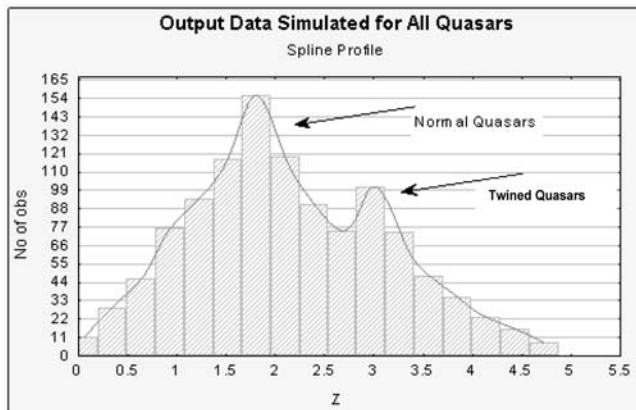


Fig. 6. Observed double peak shape in  $Z$  quasars distribution like in fine theoretical models [21]

5) The fifth process prepares the trapping and performs the trapping and guiding of light in the channels.

6) The sixth process tests that the same light ray is not counted more than one time if it intersects more subcylinders of the same channel.

The results of the simulation are summarized below, by considering: 1) a fixed number of waveguides chosen in relation to  $R_i$  for the planar case and 5000 for the filamentary one; 2) 10000 quasars randomly fixed as input.

a) The quasar positions  $R$  (in Mpc) and the redshifts  $Z$ , after the attenuation, have a Gaussian distribution and fit with the mean value and the standard deviation in full agreement with theoretical and observational results [8, 19, 20].

b) Also for twinned quasars,  $R$  and  $Z$  are comparable with the theoretical models; in particular, twinned quasars are a subset of the input quasars and they are also isotropically distributed.

About 10% of initial quasars pass through the attenuation process. A fraction, from 10 to 35% of quasars after the attenuation, undergoes the channeling effect. This fraction is linked to the number of channels. The number of twinned quasars increases with the number of channels, by fixing the number of quasars after the attenuation. A preliminary fit can be made between the number of refraction channels and twinned quasars. The results are in full agreement with filamentary channels. In fact, about 10% of the initial quasars pass through the attenuation process, and a fraction of

about 14% of these ones undergoes the channeling effect.

Our analysis shows two peaks in the distribution of quasars: the higher one is due to nontwinned quasars, whose light is not trapped and guided in the channels, and the shortest is due to twinned quasars. This fraction is in the range 10–35% (Fig. 6).

## 5. Discussion and Conclusion

In this paper, we consider an alternative and complementary mechanism respect to the lensing effect due to the waveguiding effect. In nature, this effect happens when light pass through a field that is generated by a matter distribution. Probably, this point of view is more realistic respect to a single point-like lens<sup>3</sup>. This work generalizes the idea presented in [7, 8] to give a mechanism by which it is possible to explain two of the major puzzles of quasar theory: the huge luminosity and the twin (or brother) objects. Both of them, till now, have invoked exotic explanations as the presence of a supermassive black hole inside the core radius or lensing effects, where the position and size of an intervening deflector (usually, a galaxy) have to be “finely tuned” in the same sense. The huge luminosity at a far red-shift is nothing else but the effect of the channel which “draws” the luminosity of the source closer to the observer. This fact means that the source brightness will turn out to be much stronger than the brightness of analogous objects located at the same distance (i.e. at the same redshift  $Z$ ) and the apparent energy released by the source seems anomalously large.

In addition, the large angular distance separation of twins and brothers is due to the geometry of (filamentary or planar) channels without posing “ad hoc” lens galaxies between the source and the observer. This hypothesis, as shown, naturally explains the double-peak luminosity function of quasars.

Respect to this paper, it could be interesting to investigate the link with the fractal universe model and waveguiding effects more in detail, as well as the scale relativity.

The authors wish to thank S. Capozziello for suggestions.

1. *Schneider P., Ehlers S., Falco E.E.* Gravitational Lenses. — Berlin: Springer, 1992.

<sup>3</sup>To be more precise, many lens models exist, but the point of view is the same of a single point-like lens: light is outside of the deflector and no channeling effects are considered.

2. *Bliokh P.V., Minakov A.A.* Gravitational Lenses. — Kyiv: Naukova Dumka, 1989 (in Russian).
3. *Fan. X, White R.L. et al.* [astro-ph/0005414].
4. *Zheng W., Tsvetanov Z.I. et al.* [astro-ph/0005247].
5. *Vilenkin A.* // Ap J., **282** (1984) L51.
6. *Vilenkin A.* // Phys.Repts., **121** (1985) 263.
7. *Capozziello S., Iovane G.* // Grav. Cosm. **5**, N 1 (1999) 17.
8. *Capozziello S., Iovane G.* // A&A **366**, N 3, Feb. II (2001) 736.
9. *Connes A.* Noncommutative Geometry. — New York: Academic Press, 1994.
10. *El Naschie M.S.* // Chaos, Solitons and Fractals. **9**, N 10 (1998) 1789.
11. *Mackay A.* // Physica A, **114** (1982) 609.
12. *Man'ko V.I.* // Lee Methods in Optics: Lecture Notes in Physics / Ed. by Mondragon & Wolf, **250** (1986) 193.
13. *Kibble T.V.B.* // J.Phys.A, **9** (1976) 1387.
14. *Gott III J.R.* // ApJ, **288** (1985) 422.
15. *Vachaspati T., Vilenkin A.* // Phys.Rev.Lett., **67** (1991) 1057.
16. *Kolb E.W., Turner M.* Early Universe. — New York: Addison-Wesley, 1990.
17. *Sylos Labini F., Montuori M., Pietronero L.* // Phys.Repts., **293** (1998) 61.
18. *National Instruments*, 2003, Labview 7 Express.
19. *Fort B., Mellier Y.* // A&A, **5** (1994) 239
20. *Broadhurst T.J., Taylor A.N., Peacock J.A.* // ApJ, **438** (1995) 49.
21. *CRONARIO coll.*, 1998, internal communication.

Received 08.07.03.

#### НИТКОПОДІБНА І ПЛОСКА СТРУКТУРИ У ГРАВІТАЦІЇ ТА СПОСТЕРЕЖУВАНІ ЕФЕКТИ

*Г. Іоване, Е. Лазерра*

#### Резюме

Розглянуто ефект хвилеводу стосовно великомасштабної структури Всесвіту. Зокрема, вважається, що ниткоподібна і плоска великомасштабні структури є можливими каналами рефракції для електромагнітного випромінювання, що йде від космічних структур. Шляхом комп'ютерного моделювання на основі цієї гіпотези і аналітичної моделі вдалося пояснити розподіл світимості квазарів і, зокрема, наявність “близнюків” та “братів”. Детально описано метод моделювання.